Conf-830805--9

CONF-830805--9

DE83 009625

Analytical Response of Concrete Structures Subjected to High Temperatures

A. H. Marchertas and J. M. Kennedy
Argonne National Laboratory

DISCLAIMER

This report was prepared as an account of work sponsored by an agency of the United States Government. Neither the United States Government nor any agency thereof, nor any of their employees, makes any warranty, express or implied, or assumes any legal liability or responsibility for the accuracy, completeness, or usefulness of any information, apparatus, product, or process disclosed, or represents that its use would not infringe privately owned rights. Reference herein to any specific commercial product, process, or service by trade name, trademark, manufacturer, or otherwise does not necessarily constitute or imply its endorsement, recommendation, or favoring by the United States Government or any agency thereof. The views and opinions of authors expressed herein do not necessarily state or reflect those of the United States Government or any agency thereof.

NOTICE
PORTIONS OF THIS REPORT ARE ILLEGIBLE.
It has been reproduced from the best available copy to permit the broadest possible availability.

MASTER
DISTRIBUTION OF THIS DOCUMENT IS UNLIMITED

Summary

Scenarios of nuclear reactor safety consider the possibility that structural concrete may be subjected to very high temperatures and thus raise the concern of containment integrity. This paper describes the analytical models and numerical tools that were developed for the purpose of studying the high temperature behavior of concrete. A formulation for computing heat conduction and stress analysis is presented and incorporated into the computer code TEMP-STRESS. The code was used to simulate the high temperature concrete response of an existing experiment. Improvements to the analytical model, which represent current research efforts, are also presented.

1. Introduction

In the nuclear industry concrete is being heavily utilized not only as a structural material, but also as a principal component of radiation shielding. In fact, because of its low cost, concrete has become an indispensible part of reactor construction. Accident scenarios which involve the spillage of hot reactor coolant or even core debris on concrete surfaces concerns the overall reactor containment integrity. This basic concern has spurred investigations into the response of concrete when exposed to high temperatures and chemical attack.

It is well known that concrete is not a consistently well defined material even at standard conditions. In fact, compared to other structural materials, concrete is one of the least understood. This is understandable, bearing in mind the fact that the concrete properties depend on numerous variables such as the kind of aggregate used, its particle size, the cement/water ratio, age of concrete, etc. The method of preparation of the concrete in the field - the mixing, vibration, air entrainment and numerous other factors also contribute invariably to the variations of properties of the final product.

The deposition of hot sodium onto the surface of concrete superimposes not only the effect of excessive temperatures of the sodium, but also the likelihood of exothermic sodium-concrete chemical reactions. Under high temperatures alone the moisture would be gradually lost and material properties could change radically. Furthermore, under thermal gradients the formation of microcracks and their consolidation into finite cracks does compound the picture considerably. The uncertainty of concrete behavior under these conditions is greatly increased. The task of attempting to predict the behavior of structural concrete under these severe environmental conditions is extremely difficult.

The work described in this paper represents structural mechanics effort underway and planned at the Argonne National Laboratory (ANL) as a part of a U.S. attempt to better understand the behavior of concrete structures in liquid metal fast breeder reactor (LMFBR) plants when such structures are subjected to either sustained high temperature levels or chemical attach or a combination of these effects. This paper describes the analytical tools developed at ANL to study concrete behavior under high temperatures. The formulation of thermo-mechanical analysis developed has been incorporated into the computer code called TEMP-STRESS [1], the basic framework of which was taken from the STRAW computer code [2,3,4] while the constitutive concrete model used had been developed for the DYNAPCON code [5,6,7].

This paper also includes the description of additional research which may have a bearing on the structural response of concrete. For those specific cases, the phenomenon will be incorporated into the detailed analysis of concrete response.

2. Analytical Basis of TEMP-STRESS

The present version of TEMP-STRESS is confined to plane and/or axisymmetric geometry. The quadrilateral four-node element with one-point integration and elastic hourglass control is used in the code to represent concrete.

An explicit time integration scheme, coupled with dynamic relaxation, has been adopted in the TEMP-STRESS code for stress analysis of concrete. This choice of temporal integration was primarily dictated by the severe material nonliniarities associated with concrete behavior. The algorithm incorporated within the TEMP-STRESS code [1] involves lumped mass and capacitance matrices and solves the transient heat conduction equation and the continuum equations of motion.

The temporal derivatives of heat conduction and the equation of motion are approximated by difference formulas to obtain the following form for the nodal temperatures $\{T\}$ and accelerations $\{\ddot{d}\}$ at step i:

$$\{T\}^i = \{T\}^{i-1} + \frac{\Delta t}{c} [m]^{-1} \left(\{H^{ext}\}^i - \{H^{int}\}^i\right), \tag{1}$$

$$\{\ddot{d}\}^i = \left([m] + \frac{1}{2}\Delta t[D]\right)^{-1} \left(\{F^{ext}\}^i - \{F^{int}\}^i - [D]\{\dot{d}\}^{i-1/2}\right), \tag{2}$$

while velocities $\{\dot{d}\}$ and displacements $\{d\}$ are obtained by central different expressions

$$\{\dot{d}\}^{i+1/2} = \{\dot{d}\}^{i-1/2} + \Delta t \{\ddot{d}\}^i, \tag{3}$$

$$\{d\}^{i+1} = \{d\}^i + \Delta t \{\dot{d}\}^{i+1/2}, \tag{4}$$

and

$$[D] = \frac{2\beta_1}{\omega_{max}}[s] + 2\beta_2 \omega_{min}[m], \tag{5}$$

where Δt is the time step, c is the specific heat, $[m]$ is the lumped mass matrix. The diagonal damping matrix $[D]$ was introduced into the equation of motion to facilitate dynamic relaxation, where β_1 and β_2 are the damping ratios for the highest and lowest mesh frequency, respectively, and ω_{max} and ω_{min} are the maximum and minimum circular frequencies of the mesh, respectively, and $[s]$ is the current diagonal stiffness matrix whose terms are approximate 'nodal stiffnesses' during the time increment Δt. The 'nodal stiffnesses' for the j-th degree-of-freedom are approximated by

$$s_j = |\Delta F_j^{int}/\Delta d_j| . \tag{6}$$

The minimum circular frequency is computed from an approximate Rayleigh quotient [8], and the maximum circular frequency is related to the critical time step for the mesh as follows

$$\omega_{min} = \sqrt{\sum_{j=1}^{N} s_j d_j^2 \Big/ \sum_{j=1}^{N} m_j d_j^2}, \qquad \omega_{max} = \frac{2}{\Delta t_{cr}}, \tag{7}$$

where N is the total number of degrees of freedom and Δt_{cr} is the critical time step of the mesh.

The external mechanical loads $\{F^{ext}\}$ and those due to thermal effects $\{H^{ext}\}$ are handled by computer code through boundary nodes. The thermal and mechanical internal forces are element-dependent and are derived as follows

$$\{H^{int}\} = k \int_V [B]^T [B] dV \{T\}, \tag{8}$$

$$\{F^{int}\} = \int_V [B]^T \{\sigma\} dV \ , \tag{9}$$

where k is the thermal conductivity, V is the volume of the element and $\{\sigma\}$ is the element stress matrix. The [B] matrix relates the strain $\{\varepsilon\}$ of the element to nodal displacements $\{d\}$, or the velocity strain $\{\dot{\varepsilon}\}$ of the element to the nodal velocities $\{\dot{d}\}$, as

$$\{\dot{\varepsilon}\} = [B] \{\dot{d}\} \ . \tag{10}$$

The sequence of computations programmed within the TEMP-STRESS code is the following

START
INPUT

NODAL EXTERNAL FORCES	(LOADING ACCORDING TO INPUT)
NODAL TEMPERATURES	eq. (1)
NODAL EXTERNAL TEMPERATURES	eq. (8)
ELEMENT VELOCITY STRAINS	eq. (10)
ELEMENT STRESSES	(ACCORDING TO CONSTITUTIVE MODEL)
NODAL INTERNAL FORCES	eq. (9)
NODAL DAMPING FORCES	eq. (5)
NODAL ACCELERATIONS	eq. (2)
NODAL VELOCITIES	eq. (3)
NODAL DISPLACEMENTS	eq. (4)

OUTPUT
$t^{i+1} = t^i + \Delta t$
END

The maximum value of the time step is controlled by a stability criterion which depends on the discretization of the model and material properties [1].

In the thermo-mechanical explicit integration problems involving cracking, one must be aware of several considerations. First, to make the thermal solution consistent with that of the structural solution, the real time of the problem should be reduced. This makes the thermo-mechanical solution very efficient, but should not affect its accuracy [1]. Secondly, because of cracking and the corresponding sudden drop of stress within elements, static equilibrium is violated immediately after cracking. The system must be brought back to static equilibrium before subsequent cracking can be permitted to continue. For this reason, the present version of TEMP-STRESS ascertains that the kinetic energy of the system after cracking is lower than that before cracking.

3. Sample Solution

A typical solution is described here to illustrate the current capability of the TEMP-STRESS code.

Two basalt concrete cylinders [9], identical in all respects except for the degree of constraint on the outside of the cylinder, are analytically examined here. The two concrete configurations considered are shown in Fig. 1. Figure 1a illustrates the initial configuration of the free (unconstrained) test specimen, while Fig. 1b shows another specimen (constrained) enclosed by a 30.48 cm diameter Schedule 40 steel pipe. The instrumentation used in both of the specimens is shown in Fig. 1b.

The analytical model of the concrete specimen used in this study was subdivided into finite elements as shown in Fig. 2. Because of symmetry only one-half of the specimen is modeled. In order to account for the effect of the steel jacket shown in Fig. 1b, an external force directed radially inward, representing the cylindrical membrane shell constraint is exerted on the radial boundary of the analytical model shown in Fig. 2. Temperature dependent material properties of basalt concrete and steel constraint were used in this example [10].

Figure 3 shows the thermocouple readings of the free concrete cylinder given in Fig. 1a. It may be noted that a sharp temperature rise is indicated by the 1 cm thermocouple at about 20 min and a similar deviation is shown at about 35 min by the 2.5 cm thermocouple. This sharp temperature rise represents the effects of an exothermic chemical reaction and is indicative of the advancement of the sodium-concrete interface during the test. Figure 4 gives the corresponding temperature distributions for the model with the constraint of the steel cylinder. Here, sharp deviations of the test temperature readings for the 1 cm and the 2.5 cm thermocouples occur at about 70 min from the initiation of the test.

Analytical temperatures for all three models are also plotted on Figs. 3 and 4. The assumed surface temperature was derived by matching the experimental and the analytical temperatures. These analytical temperatures illustrated in Figs. 3 and 4 thus provide loadings to which each of the analytical models are subjected.

Figure 5 depicts the cracking history of the unconstrained model. Cracking originates inside the body of the cylinder as early as 3 min. Propagation occurs in a nonuniform fashion contrary to what may be expected for a rather uniform heating. The cracking is predominantly conical-circumferential. A certain amount of radial cracking initiates at the upper outside boundary and spreads inward.

The cracking patterns for the constrained model are shown in Fig. 6 extending through 70 min. Although the first crack is indicated at 4 min, significant crack propagation is not indicated until about 10 min. Afterwards, the cracking proceeds in a similar nonuniform fashion as in the free model, but at a slower rate. Here cracking is solely conical-circumferential.

The structural solution shown does not yield any quantitative results to help explain the experimentally observed differences between the free and constrained test models. Apparently the phenomenon responsible for the observed differences is not modeled within the TEMP-STRESS code. The primary requirement of significant surface erosion is the threshold temperature, but there must exist some other as yet unknown parameter which triggers the rapid phase of erosion. An attempt is being made to explain the apparent effect of constraint.

One important influence may be the thermal shrinkage of concrete caused by dehydration. It has been established that the cement paste shrinks excessively when heated from 300°C to 850°C. It is also known that the surface of concrete is richer in mortar than the main body of concrete [11]. Because thermal shrinkage competes with thermal expansion, distress is created in the microstructure causing a drop in material strength. Confinement would impede both the expansion and the shrinkage of the test specimen.

The breaking-up of the surface due to thermal differential expansion between the mortar and aggregate might be another mechanism which could explain the threshold of rapid surface erosion [11]. External constraint could restrict the amount of this local relative displacement. On the other hand, if the object is permitted to expand unobstructed, then the thermally induced relative displacement between mortar and aggregate could reach some critical limit and hence rupture the bond between the materials.

4. Current Research on Concrete Modeling

The important parameters in the response of concrete under high temperatures concerns cracking, creep, shrinkage, spalling, possible surface erosion, not to mention the variables involved of concrete interaction with the steel reinforcement. Of equal importance in this research effort are the mechanical and thermal properties which change with temperature and loss of moisture. Constitutive models for concrete are being explored for implementation into the code. Algorithms for crack propagation, creep phenomenon, pore pressure and moisture migration are also being developed.

Of paramount concern in direct thermal attack of concrete by hostile environments (such as hot sodium coolant) is the formation of cracks, which complicates the analysis considerably. In previous simulations cracking was approximated by the maximum principal stress criterion. Recent efforts involve the prediction of crack propagation using the energy release rate of concrete. This approach minimizes the element-size effect of the analytical finite element models. The new approach is presently undergoing close scrutiny.

Creep is another parameter which may significantly affect concrete behavior at very high temperatures. It is also known that creep is dependent on the loss of moisture from concrete. In order to estimate the significance of high temperature creep in stress analysis we must know, therefore, not only the temperature but also the water content. An estimate of the water content at high temperature can be obtained from already available water release codes. Most of these codes are limited to 1-D geometry so that additional modifications are still needed. Better confidence in material properties, such as the permeability of concrete, must also be established.

Using experimentally verified water release codes, an approximation of concrete creep will be made. Initially the effective modulus method will be used to study the significance of high temperature concrete creep. A by-product of the moisture release codes is the calculation of the pore pressure distribution. Knowledge of pore pressure may help in the search for the cause of concrete surface spalling. Futhermore, because shrinkage is approximately proportional to the water loss, the integral effect of drying shrinkage could be approximated from the water content.

5. Final Remarks

Lumped mass-capacitance calculations coupled with explicit integration provide a very convenient method of calculating thermal stress. The dynamic relaxation solution strategy is quite efficient not only for transient but also for steady state problems. There are also by-products of the explicit integration scheme which are very important. For example, this procedure provides a detailed cracking sequence simulation, which is essential in the history-dependent problems such as cracking propagation. The very simple coding architecture is another by-product of this approach which is of great significance to the code developer. Computations are also economical, because the thermal part consumes only about 20% of the total time. This figure is based on one integration per element for structural calculations and one integration per element for conductance calculations.

With the objective of better understanding of concrete behavior under high temperature and ultimately under sodium-concrete or for core debris-concrete reactions, we plan to incorporate other relevant variables into our models, such as creep, an updated constitutive model for concrete, the equivalent strength criterion or other improved representation of cracking, etc. The overall importance of each individual parameter to the modeling of concrete will be the controlling factor; a permanent addition to the TEMP-STRESS code will be made when such importance of the specific parameter to the response of concrete is well established, and understood.

Acknowledgement

This work was performed in the Engineering Mechanics Program of the Reactor Analysis and Safety Division at Argonne National Laboratory, under the auspices of the U.S. Department of Energy.

References

[1] A. H. Marchertas and R. F. Kulak, "A Coupled Heat Conduction and Thermal Stress Formulation Using Explicit Integration," Argonne National Laboratory Report, ANL-82-47, June 1982.

[2] J. M. Kennedy, "Nonlinear Dynamic Response of Reactor-Case Subassemblies," ANL-8065 (Jan. 1974).

[3] D. F. Schoeberle, J. M. Kennedy and T. B. Belytschko, "Implicit Temporal Integration for Long-Duration Accidents in a Structural Response Code - STRAW," ANL-8136 (Oct. 1974).

[4] R. F. Kulak, T. B. Belytschko, J. M. Kennedy, and D. F. Schoeberle, "Finite Element Formulation for Thermal Stress Analysis of Thin Reactor Structures," Nucl. Eng. Design, Vol. 49, 39-50 (1978).

[5] A. H. Marchertas et al., "Analysis and Application of Prestressed Concrete Reactor Vessels for LMFBR Containment," Nucl. Eng. Design, 49 (1 & 2), 155-173 (1978).

[6] A. H. Marchertas and T. B. Belytschko, "Transient Analysis of a PCRV for LMFBR Primary Containments," special issue on "Mechanics Application to Fast Breeder Reactor Safety," Nucl. Technol., 51(3), 433-442 (1980).

[7] A. H. Marchertas, "DYNAPCON - A Computer Code for DYNamic Analysis of Prestressed CONcrete Structures," Argonne National Laboratory Report, ANL-82-77, September 1982.

[8] P. G. Underwood, "An Adaptive Dynamic Relaxation Technique for Nonlinear Structural Analysis," Lockheed Palo Alto Research Lab., LMSC-D678265, (1979).

[9] R. U. Acton, et al., Advanced Reactor Safety Research Quarterly Report for October-December 1980, NUREG-CR-1594 (4 of 4), Sandia National Laboratories, Albuquerque, NM, 1981.

[10] A. H. Marchertas and R. F. Kulak, "Numerical Modeling of Concrete Under Thermal Loads," Nucl. Eng. Design, 68, (2.2), 225-236 (1981).

[11] Prof. Edward C. Ting, Purdue University, June 1982, personal communication.

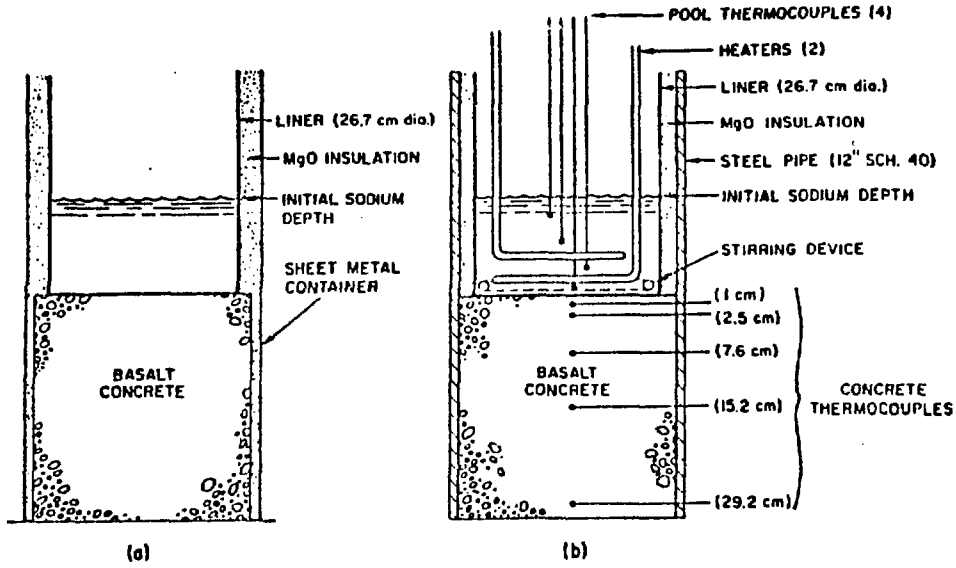

Fig. 1. Test Specimen Configurations: (a) Free Cylinder, (b) Constrained Cylinder (Courtesy of Sandia National Laboratories).

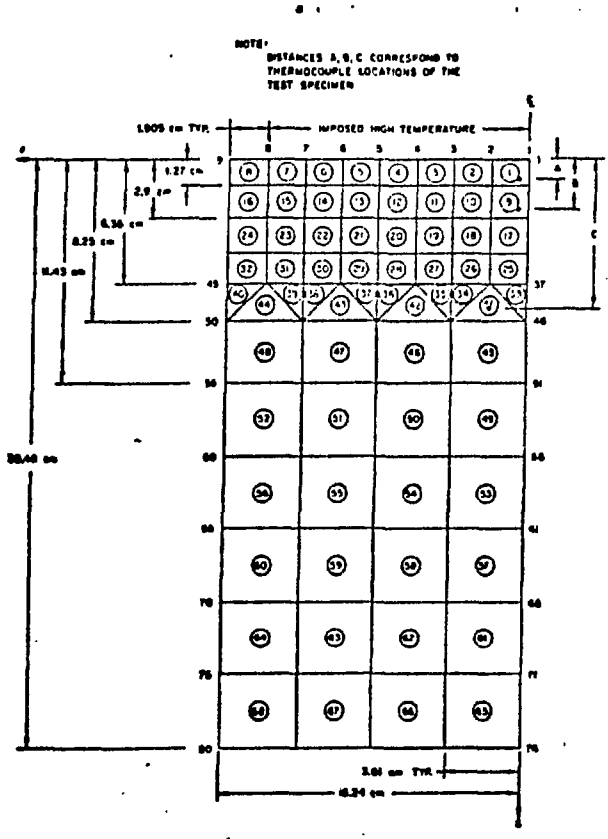

Fig. 2. Details of the Analytical Model.

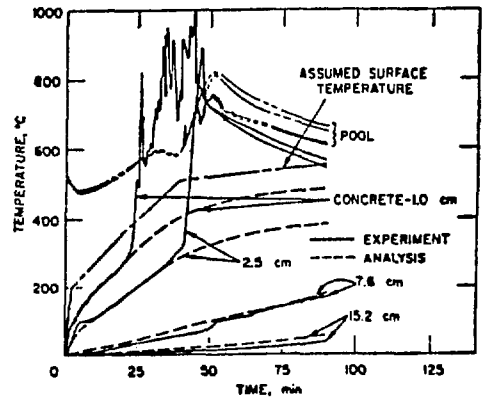

Fig. 3. Analytical and Test Temperatures in Concrete and Pool for the Unconstrained Model (Courtesy of Sandia National Laboratories).

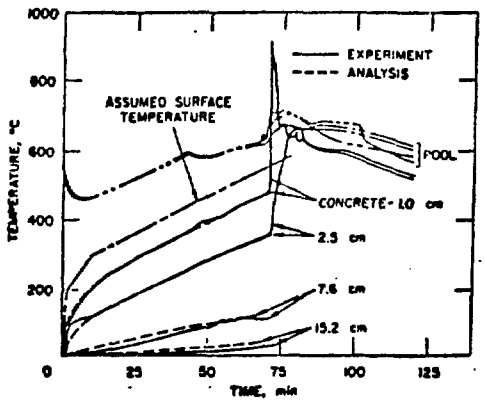

Fig. 4. Analytical and Test Temperatures in Concrete and Pool for the Constrained Model (Courtesy of Sandia National Laboratories).

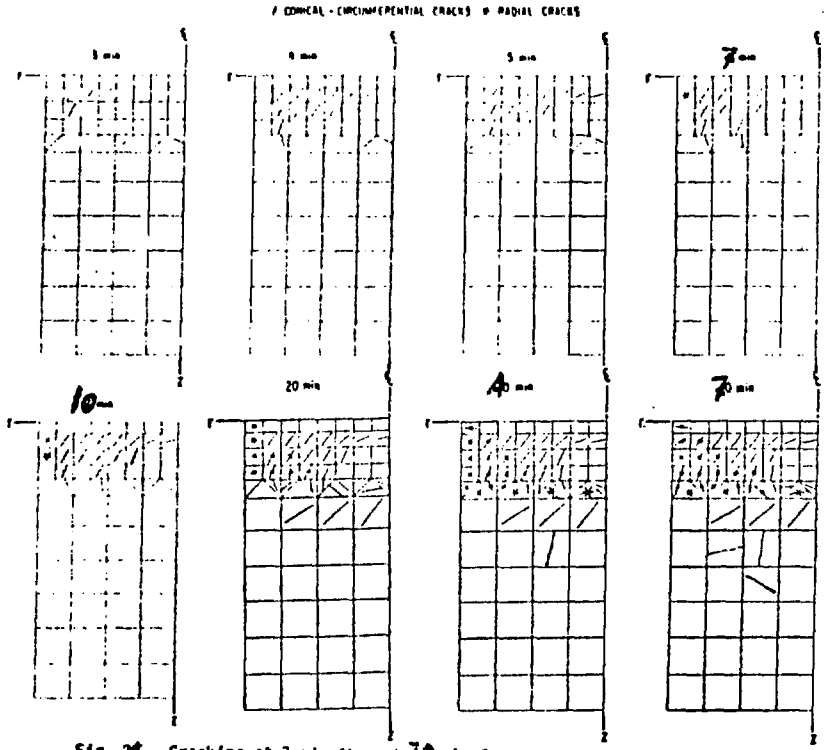

Fig. 5. Cracking at 3 min through 70 min for the Unconstrained Model.

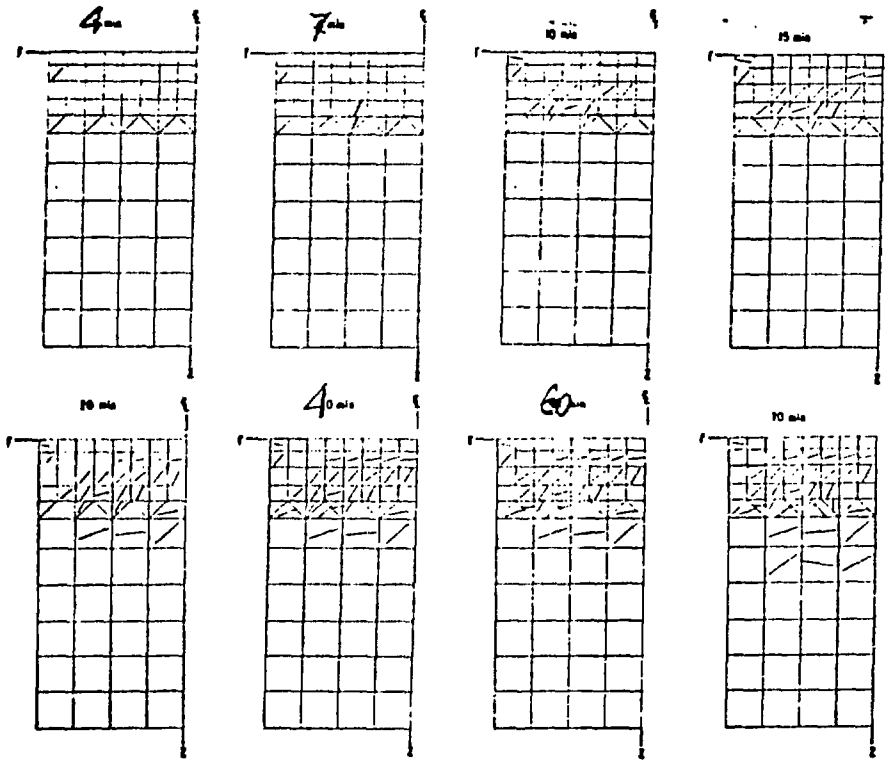

Fig. 6. Cracking at 40 min through 70 min for the Constrained Model.